
Supporting Information

Chemically Modified Ribbon Edge Stimulated H₂ Dissociation: A First-Principles Computational Study

Ting Liao,*^a Chenghua Sun,^{a,b} Ziqi Sun,^c Aijun Du^a and Sean Smith*^d

^a Centre for Computational Molecular Science, Australian Institute for Bioengineering and Nanotechnology, University of Queensland, Brisbane QLD4072, Australia.

^b ARC Centre of Excellence for Functional Nanomaterials, Australian Institute for Bioengineering and Nanotechnology, University of Queensland, Brisbane QLD 4072, Australia.

^c Institute for Superconducting & Electronic Materials, University of Wollongong, NSW 2500, Australia.

^d Centre for Nanophase Materials Sciences, Oak Ridge National Laboratory, Oak Ridge, TN 37831, USA.

Computational details:

Our numerical approach is based on the spin polarized density functional theory (DFT) using the *ab initio* pseudopotential plane-wave method as implemented in the PWSCF code.¹ The Perdew-Burke-Ernzerhof gradient corrected functional (PBE) is employed as the exchange-correlation functional.² Ultrasoft pseudopotentials have been used.³ The valence electronic wave functions were expanded onto a plane wave basis set with a kinetic energy cutoff of 40 Ryd for wave functions and 300 Ryd for charge density. For most of the calculations, a 7×1×1 Monkhorst-Pack *k*-point mesh was used.⁴ The electronic structure analysis with 35×1×1 *k*-point mesh have also been performed.

To determine the ionic oxygen diffusion barriers, transition states were determined using the nudged elastic band method (NEB).⁵ A set of intermediate configurations, or ‘images’, generated by linear interpolation between the two equivalent endpoint configurations were then optimized so as to converge to points on the minimum energy path. Harmonic spring interactions were used to connect the different images of the system along the path. Conjugated gradients algorithm is used to minimize the forces on the images.

Computational results:

The substitutional stability of heteroatoms B, N, and O on ribbon edge was examined in the supercell. The substitution energy can be addressed as

$$E_{\text{sub}} = E_{\text{heteroatom:ZGNR}} - E_{\text{ZGNR}} - \mu_{\text{heteroatom}} + \mu_{\text{carbon}} \quad (1)$$

where $E_{\text{heteroatom:ZGNR}}$ is the energy of the heteroatom-substituted supercell, E_{ZGNR} is the energy of pristine supercell, and $\mu_{\text{heteroatom}}$ and μ_{carbon} are calculated using the total energy of their ground states of each species. All substitutional processes turn out to be exothermic, -0.78, -1.17, and -2.08 eV respectively for the order of B-, N-, and O-doping, most notably for oxygen, which provides a complementary understanding of easy contamination of graphene in oxidized environments.

Based on the DFT calculation, both B- or N-doping can contribute positively to the H_2 dissociation by reducing the dissociative energy barrier, in a similar way on enhancing ORR activity from experimental and theoretical perspectives. The important role of light element doping on stimulating the H_2 dissociation reported in this work add a precious data to the various other metal-free efficient catalyst, like the oxygen reduction reaction (ORR) for fuel cell applications or beyond.

Table S1. Löwdin charge population results for B-, N, O-doped and undoped graphene ribbon during H_2 dissociation process. IS, TS, and FS represent initial structure, transition state and final structure, respectively.

B-doped	IS	TS	FS	un-doped	IS	TS	FS
Dopant	2.864	3.115	2.774	Edge C	3.835	4.077	3.958
C*	3.982	4.012/4.012	4.164/4.131	C*	4.086	4.022	4.142
H	0.964	0.743/0.789	0.799/0.886	H	0.966	0.885	0.793
N-doped	IS	TS	FS	O-doped	IS	TS	FS
Dopant	5.086	5.202	5.217	Dopant	6.074	6.191	6.348
C*	3.959	3.931	3.977	C*	3.931	3.953	3.928
H	0.967	0.871	0.795	H	0.966	0.897	0.791

Table S2. Calculated physical adsorption energy of H₂ on B-, N, O-doped and undoped graphene ribbon edges with and without van der Waals correction.

E_{ad}/eV	B-doped	Un-doped	N-doped	O-doped
without vdW	-0.0009	-0.0015	-0.0067	-0.0252
vdW correction	-0.0182	-0.0200	-0.0250	-0.0378

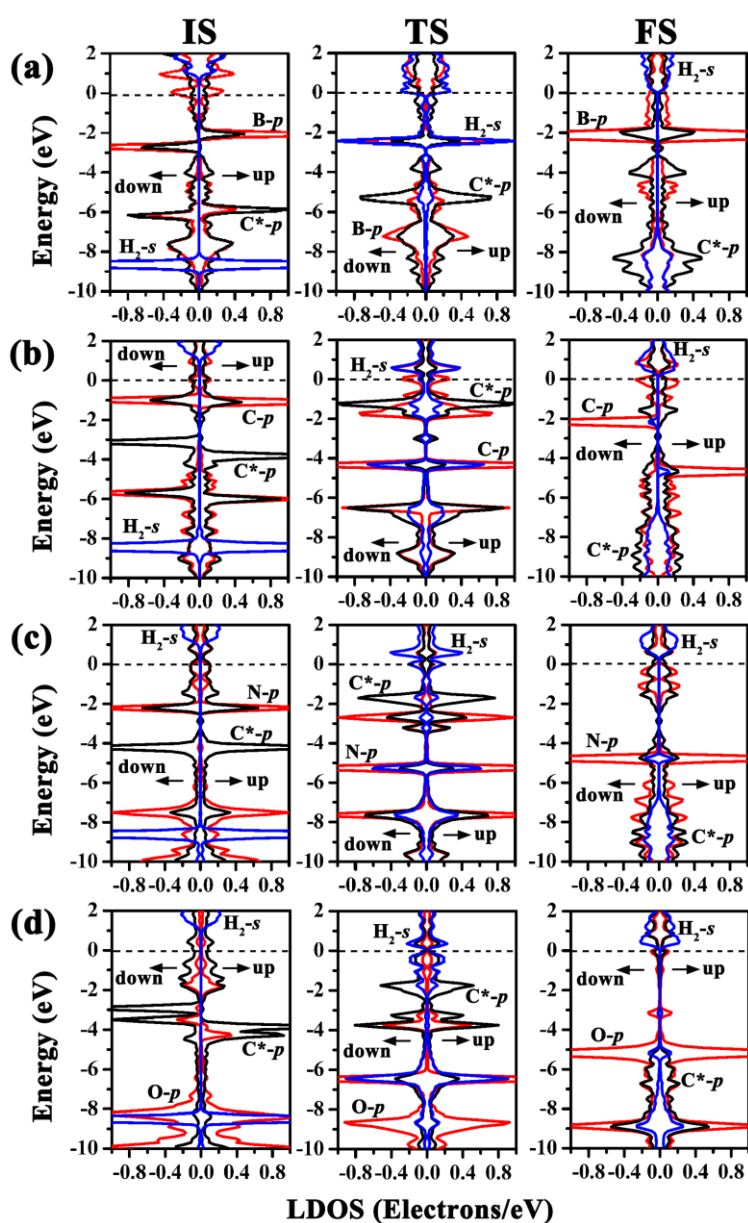


Fig. S1. Spin-polarized local density of states projected onto doped edge atom,

adsorbing site C* and H₂, in the IS, TS, and FS configurations as illustrated in Fig. 2.

The Fermi level is set to zero.

References:

- 1 S. Baroni, A. Dal Corso, S. de Gironcoli, P. Giannozzi, PWSCF (plane wave self consistent field) codes Available at: <http://www.quantum-espresso.org>.
 - 2 J. P. Perdew, K. Burke, M. Ernzerhof, *Phys. Rev. Lett.* **1996**, *77*, 3865.
 - 3 D. Vanderbilt, *Phys. Rev. B* **1990**, *41*, 7892.
 - 4 J. D. Pack, H. J. Monkhorst, *Phys. Rev. B* **1977**, *16*, 1748.
 - 5 G. Henkelman, B. P. Uberuaga, H. Jónsson, *J. Chem. Phys.* **2000**, *113*, 9901.
-